

SHRP-P-392

Early Analyses of LTPP General Pavement Studies Data

Executive Summary

J. Brent Rauhut
Brent Rauhut Engineering Inc.
8240 North Mopac, #220
Austin, Texas 78759

Michael I. Darter
ERES Consultants, Inc.
8 Dunlap Court
Savoy, Illinois 61874



Strategic Highway Research Program
National Research Council
Washington, D.C. 1994

SHRP-P-392
Contract P-020
ISBN 0-309-05774-4
Product No.: 5000

Program Manager: *Neil F. Hawks*
Project Manager: *A. Robert Raab*
Program Area Secretaries: *Cynthia Baker, Francine A. Burgess*
Production Editor: *Margaret S. Milhous*

April 1994

key words:
data analysis
pavement design
asphalt pavement
portland cement concrete pavement

Strategic Highway Research Program
National Research Council
2101 Constitution Avenue N.W.
Washington, DC 20418

(202) 334-3774

The publication of this report does not necessarily indicate approval or endorsement by the National Academy of Sciences, the United States Government, or the American Association of State Highway and Transportation Officials or its member states of the findings, opinions, conclusions, or recommendations either inferred or specifically expressed herein.

©1994 National Academy of Sciences

Acknowledgments

The research described herein was supported by Strategic Highway Research Program (SHRP). SHRP is a unit of the National Research Council that was authorized by Section 128 of the Surface Transportation and Uniform Relocation Assistance Act of 1987.

We wish to acknowledge the valuable review, discussion, and suggestions by the Expert Task Group on Experimental Design and Analysis, the Pavement Performance Advisory Committee, SHRP staff, and SHRP Contract P-001 staff. The many technical memoranda developed by Contract P-001 staff were especially valuable.

Contents

Abstract	1
Executive Summary	3
Limitations Resulting From Data Shortcomings	4
Evaluation of the AASHTO Flexible Pavement Design Equation	6
Evaluation of the AASHTO Rigid Pavement Design Equation	8
Improved Design Equations—Applications and Limitations	13
HMAC Pavements	14
PCC Pavements	17
Evaluation of the 1993 Overlay Design Equations	19
Sensitivity Analyses and Results	21
Sensitivity Analyses for HMAC Pavements	21
Summary of Sensitivity Analysis Results for HMAC Pavements	23
Sensitivity Analyses for PCC Pavements	24
Summary of Sensitivity Analysis Results for PCC Pavements	26
Tentative Conclusions for JPCP	29
Tentative Conclusions for JRCP	30
Tentative Conclusions for CRCP	30
Recommendations for Future Analyses	31

List of Figures

1.	Distribution of Pavement Age, Experiment GPS-1, HMAC Over Granular Base	4
2.	Plot of Predicted Versus Actual KESALs Based on Backcalculated Subgrade Moduli for 244 Test Sections	9
3.	Plot of Predicted Versus Actual KESALs Based on Subgrade Resilient Moduli From Laboratory Testing for 106 Test Sections	9
4.	Predicted KESALs Versus Actual KESALs for JPCP and JRCP Determined With the Original AASHTO Prediction Model	11
5.	Predicted KESALs Versus Actual KESALs for JPCP, JRCP, and CRCP Determined With the 1993 AASHTO Prediction Model	12
6.	Design Nomograph to Limit Roughness in the Dry-Freeze Zone	15
7.	Results From Sensitivity Analyses for Rutting in HMAC on Granular Base	22
8.	Sensitivity Analysis for Doweled Joint Faulting Model	26
9.	Three-Dimensional Plot (FAULTD, AGE, CESAL) of Doweled Joint Faulting Model	27
10.	Three-Dimensional Plot (FAULTD, JTSPACE, CESAL) of Doweled Joint Faulting Model	27

List of Tables

1.	Predicted Change in Roughness in In./Mi. Based on Regional Predictive Equations, Ranges of Layer Thicknesses and ESALs, With Climatic Data at Their Regional Means, HMAC Over Granular Base (Also Predictive Equation Statistics)	16
2.	Use of LTPP Predictive Models for Evaluating a JRCP Design Example	18
3.	Results From Comparative Evaluation of 1993 AASHTO Overlay Equations	20
4.	Coefficients for Regression Equations Developed to Predict Rutting in HMAC on Granular Base for the Wet-Freeze Data Set	22
5.	Significance Rankings for Explanatory Variables, by Distress Type and Pavement Type, for PCC Pavements	28

Abstract

This Executive Summary presents the results from the first analyses of the SHRP Long-Term Pavement Performance (LTPP) data collected up to 1992. These analyses included (1) developing a data analysis plan, (2) receipt and processing of data into suitable databases for analysis and conducting statistical evaluations of the databases, (3) using the LTPP data to evaluate the American Association of State Highway and Transportation Officials (AASHTO) design equations, (4) conducting sensitivity analyses to identify the independent variables that have significant impacts on pavement performance and to quantify the relative impact of each, and (5) using the experience gained from these early data analyses to recommend concepts for future data analyses.

Executive Summary

The first analysis of the Strategic Highway Research Program (SHRP) Long-Term Pavement Performance (LTPP) data has been completed on data collected up to 1992. Brent Rauhut Engineering Inc. conducted the flexible pavement analyses, and ERES Consultants, Inc., the rigid pavement analyses. This effort was funded by SHRP Contract P-020, "Data Analysis." SHRP's objectives in this contracted research work were (1) to develop and implement a strategic approach to the analysis of LTPP data to support the overall goals of SHRP and LTPP and (2) to develop data analysis plans for LTPP data to be followed in the future.

In order to accomplish these objectives, the contractors conducted the following activities: (1) developed a data analysis plan in coordination with the SHRP-Federal Highway Administration Pavement Performance Advisory Committee and the Expert Task Group on Experimental Design and Analysis, (2) received and processed data into suitable databases for analysis and conducted statistical evaluations of the databases, (3) used the LTPP data to evaluate the American Association of State Highway and Transportation Officials (AASHTO) design equations, (4) conducted sensitivity analyses to identify the independent variables that have a significant impact on pavement performance and to quantify the relative impact of each, and (5) used the experience gained from these early data analyses to recommend concepts for future data analyses.

A number of databases were formed, each representing a combination of distress type and pavement type. The statistical evaluations of the separate databases provided characterizations of the data within the databases and identified shortcomings in the data. This information will allow future analysts to overcome some of these shortcomings.

Most important, the potential value of the LTPP database was demonstrated through development of many key distress and roughness models and through the evaluation of the AASHTO Design Guidelines. These results, limited as they are, demonstrate the high potential of the LTPP database.

Limitations Resulting From Data Shortcomings

The General Pavement Studies (GPS) involved the analysis of data observed on in-service pavements. These early results depend on the adequacy of the database from which they are developed. Therefore, certain limitations to the studies are unavoidable because of the timing of the early data analyses. For instance, although much better traffic data will be available for future analysts from recently installed monitoring equipment, these early data analyses were based on estimates of past equivalent single axle loads (ESALs) of limited accuracy. While years of time sequence monitoring data will be available later, these studies had distress measurements for only one point in time. For most distresses, an additional data point could be inferred for conditions just after construction; for example, rutting, cracking, faulting of joints, etc., were generally taken as zero initially. Analyses for increases in roughness depended for most test sections on educated estimates for initial roughness (derived from State Highway Agency [SHA] estimates of initial Pavement Serviceability Index [PSI]). Similarly, the evaluations of the AASHTO design equations also depended on the SHA estimates of initial PSI.

The distribution in ages of the LTPP sections offered some assistance in overcoming the lack of time sequence data. As an example, Figure 1 shows the distribution of pavement ages for the GPS-1 experiment, Asphalt Concrete Over Granular Base. A number of test sections are represented in all time intervals through 20 years of age.

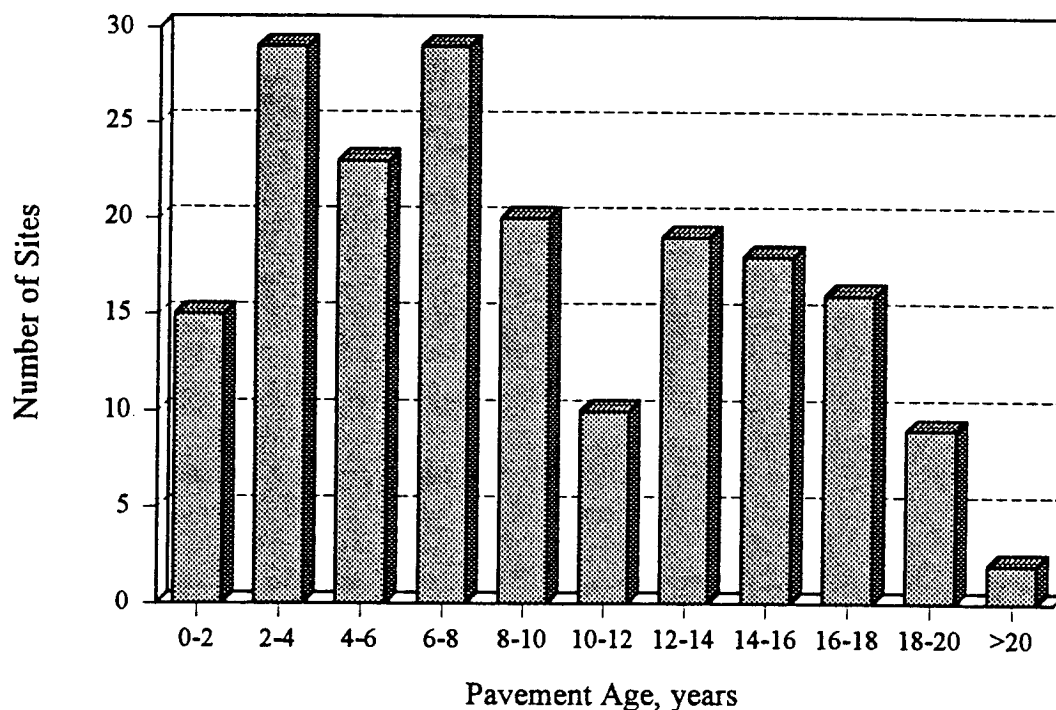


Figure 1. Distribution of Pavement Age, Experiment GPS-1, HMAC Over Granular Base

Another shortcoming that influenced the results were missing data from SHA project files on the design and construction of the pavements. Some data elements were available for all the test sections, while for others test sections data were not known and could not be found. Unfortunately, it will generally not be possible to obtain these missing inventory data so they will be missing from future analyses as well.

Many of the test sections had not yet experienced distresses, and those that had generally had only one or two distress types. The only type of distress available for essentially all test sections was roughness, but it was necessary to estimate the initial roughness for each test section in order to study increases in roughness. For flexible pavements, rutting information was also available for nearly all test sections. It was not possible to study alligator cracking in flexible pavements because only eighteen test sections reported having any alligator cracking. Similarly, raveling and weathering could not be studied because only three test sections had experienced this distress. The only three distress types for flexible pavements for which sufficient data were available to support the studies were rutting, change in roughness (measured as International Roughness Index [IRI]), and transverse (or thermal) cracking.

Predictive models for portland cement concrete (PCC) pavements were developed for ten combinations of pavement type and distress type. The models include joint faulting for doweled and non-doweled joints; transverse cracking for jointed plain concrete pavement (JPCP); transverse crack deterioration for jointed reinforced concrete pavement (JRCP); joint spalling for JPCP and for JRCP; and roughness for doweled JPCP, non-doweled JPCP, JRCP, and continuously reinforced concrete pavement (CRCP). However, sufficient data were not available to allow development of regional models, because the number of total test sections that could be used for a specific combination of pavement type and distress varied only from 21 to 59. However, more distress may be expected for future analyses, and it will appear as a number of data points over time.

The study of overlaid pavements was of high priority. However, pavement condition before overlay was an important variable, and this information was not available for pavements that were overlaid before the GPS. It was decided early in the implementation of the LTPP studies that test sections would be sought for pavements for which overlays were imminent, so that knowledge of the condition before overlay would be available. A number of such test sections have been included, but none of those were old enough to have appreciable distress. The total number of overlaid pavements was limited, and, for the reasons discussed above, only a few had sufficient information for successful analyses. Consequently, analyses for the overlaid pavements have been limited to evaluating the 1993 AASHTO overlay design equations. More overlaid test sections and more distresses will be available for future studies.

Evaluation of the AASHTO Flexible Pavement Design Equation

The equation evaluated was the one in the 1986 AASHTO Guide for Design of Pavements:

$$\log W = Z_R * S_o + \frac{G_t}{\beta} + 2.32 \log M_r - 8.07 \quad (1)$$

where	G_t	=	$\beta (\log W - \log \rho) = \log(\Delta \text{PSI}/2.7)$
	W	=	the number of 18 kip ESALs
	ρ	=	$0.64 (\text{SN} + 1)^{9.36}$
	β	=	$0.4 + 1094/(\text{SN} + 1)^{5.19}$
	SN	=	$a_1 D_1 + a_2 D_2 m_2 + A_3 D_3 m_3 + \dots + a_n D_n m_n$
	D_i	=	thickness of layer i , in.
	a_i	=	structural coefficient for the material in layer i
	m_i	=	drainage coefficient for the material in layer i
	Z_R	=	standard normal deviate
	S_o	=	overall standard deviation
	M_r	=	resilient modulus (psi) of subgrade

Because this equation was used for research instead of for design, a 50% reliability was assumed, which resulted in $Z_R = 0$.

The original equation for calculating current Pavement Serviceability Index (PSI) was reported in the American Association of State Highway Officials Road Test Report 5 as follows:

$$\text{PSI} = 5.03 - 1.91 \log (1 + \overline{sv}) - 1.38 \overline{rd}^2 - 0.01 \sqrt{c+p} \quad (2)$$

where	\overline{sv}	=	the average slope variance as collected with the CHLOE profilograph
	\overline{rd}	=	the average rut depth based on a 4 ft straight edge
	c	=	the square feet of Class 2 and Class 3 cracking per 1000 ft ²
	p	=	bituminous patching in square feet per 1000 ft ²

This equation, commonly used in the past for estimating PSI, was used to determine current PSI with values of slope variance derived from surface profiles measured with a GM profilometer and rut depths measured by PASCO's RoadRecon units. Cracking and patching were not included in the calculation of the current PSI. Significant quantities of cracking and patching were noted on only a few of the test sections, and the impact of this term was not considered significant, considering that its coefficient is only 0.01. The mean value of current PSI was 3.53, with a standard deviation of 0.49.

Observed PSI loss was then the difference between the initial PSI and the current PSI, calculated using Equation 2 above. The mean value for observed PSI loss was 0.70 and the standard deviation was 0.51. Initial values of PSI were estimated by the State Highway Agencies, resulting in a mean value of 4.25 and a standard deviation of 0.23.

Equation 1 was used to predict the total KESALs (1000 ESALs) required to cause the observed losses in PSI.

Resilient moduli for the subgrade (M_r) were represented by the stiffnesses backcalculated with the recommendations in the 1986 Guide, which are based on use of deflections measured by an outer sensor of a falling weight deflectometer. Historical traffic data provided by the SHAs were used for the traffic data (W) in these calculations. The cumulative KESALs for each section were divided by the number of years since the test section was opened to traffic to obtain average values per year. This step allowed extrapolation of the extra year or two beyond 1989 to estimate a traffic level associated with the dates of monitoring activities. Most of the monitoring data used were obtained in 1990 or 1991.

The KESALs predicted by Equation 1 were consistently *much higher* than those estimated by the SHAs (see Figure 2). Only 9 of the 244 predictions were lower than the SHA estimates, and for 112 test sections the predictions were over 100 times the SHA estimates. Because the predictions from the design equation appeared to be poor for in-service pavements, the thrust of the research turned toward identifying its problems and developing more reliable equations.

As a partial explanation, it was noted that 74% of the in-service test sections in this study had experienced a loss in PSI of 1 or less, whereas those at the road test experienced losses of 2 to 3. Further, the average absolute deviation of observed PSI from the computed curves at the AASHO Road Test was 0.46, so some 39% of the in-service test sections in this study had experienced losses of PSI within the "noise" at the Road Test.

Linear regressions were conducted on the database, based on the form of Equation 1. This resulted in an R^2 of 0.09, which indicates that the equation form simply did not represent in-service pavement performance. Additional factorial studies indicated that the equation appears to falter for structural numbers of less than 3, cumulative traffic greater than 5 million ESALs, or subgrade moduli greater than 10,000 psi (a laboratory test value of 3000 psi was used for the analyses of the Road Test data); that is, for conditions outside the inference space of the AASHO Road Test.

Linear regressions were also conducted on the ratios of predicted to observed traffic to identify which parameters might explain the lack of fit. A model with an R^2 of 0.77 resulted, which included structural number, subgrade modulus, and PSI loss (variables found in Equation 2), but also included average annual rainfall and average number of days below freezing. Attempts have been made through the years to extrapolate the equation outside its inference space, but these have apparently been unsuccessful.

The backcalculated subgrade moduli appeared to be quite high, but laboratory testing for resilient moduli was just beginning when these analyses were conducted. However, comparisons for 106 test sections for which laboratory results were available late in the analyses indicated that the mean ratio of backcalculated to laboratory-derived moduli was 4.48, with a standard deviation of 2.47. These 106 laboratory moduli were substituted for the backcalculated moduli, and the ratios of predicted to observed ESALs were considerably decreased (see Figure 3). The number of reasonable predictions (with ratios of 2 or less) changed from 6.6% based on the backcalculated subgrade moduli to 57% based on the laboratory moduli. While the predictions improved greatly, the ratios for 46 predictions still ranged from 2 to over 100, corroborating the weaknesses in the equation noted throughout the studies. It appears certain that future design equations must take into account differences between backcalculated and laboratory-derived resilient moduli.

Other limitations of the flexible pavement design equation were noted:

- The accelerated trafficking to failure at the Road Test was not representative of in-service pavements. Pavement engineers typically intercede with overlays or other rehabilitation long before serviceability loss approaches the levels considered to be at failure in the Road Test.
- The subgrade elastic moduli were assumed to be 3000 psi for the development of equations at the Road Test, whereas much higher moduli result from backcalculation procedures, and considerably higher moduli also result from current laboratory protocols.

Evaluation of the AASHTO Rigid Pavement Design Equation

The analyses were carried out using the original AASHTO design equation and the 1986 extension of the original design equation that remained unchanged in the 1993 Guide. The analysis with the AASHTO original equation was done primarily to determine if the improvements to the prediction model were beneficial.

The AASHTO design equations were evaluated for each test section by comparing the predicted 18 kip (80 kN) equivalent single axle loads (ESALs) determined from the design equation to the observed ESALs (estimated from traffic data) carried by the section. The predicted ESALs are calculated with the concrete pavement equations from the original Road Test and the latest extended form in the 1986 AASHTO Design Guide for Pavement Structures.

The original 1960 AASHTO design equation is a relationship between serviceability loss, axle loads and types, and slab thickness:

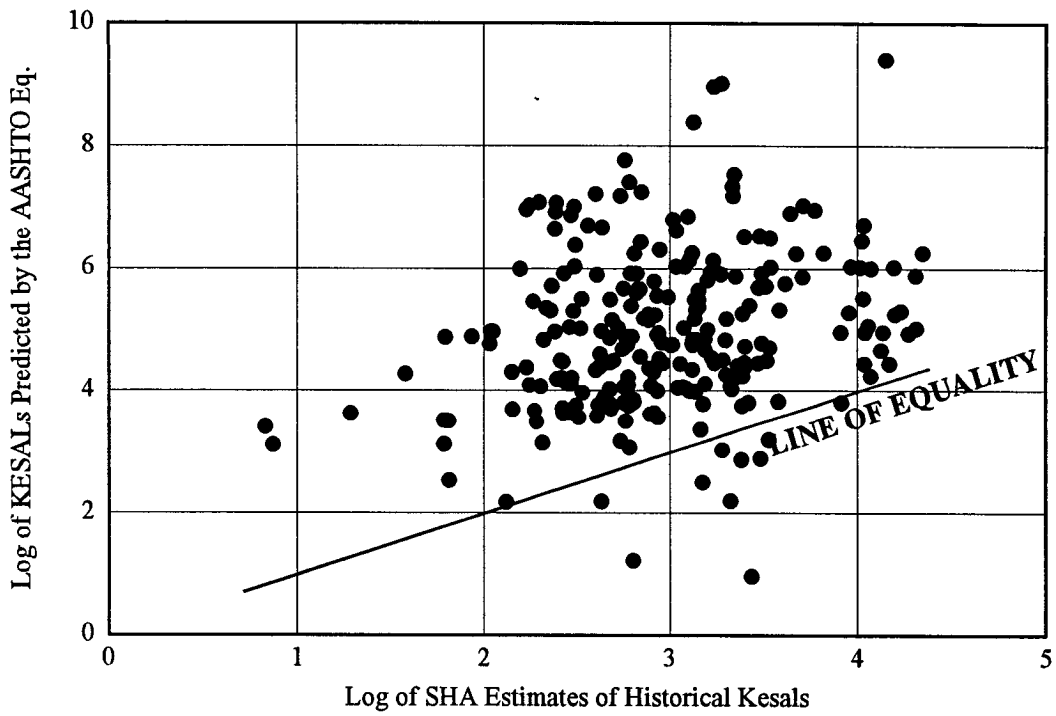


Figure 2. Plot of Predicted Versus Actual KESALs Based on Backcalculated Subgrade Moduli for 244 Test Sections

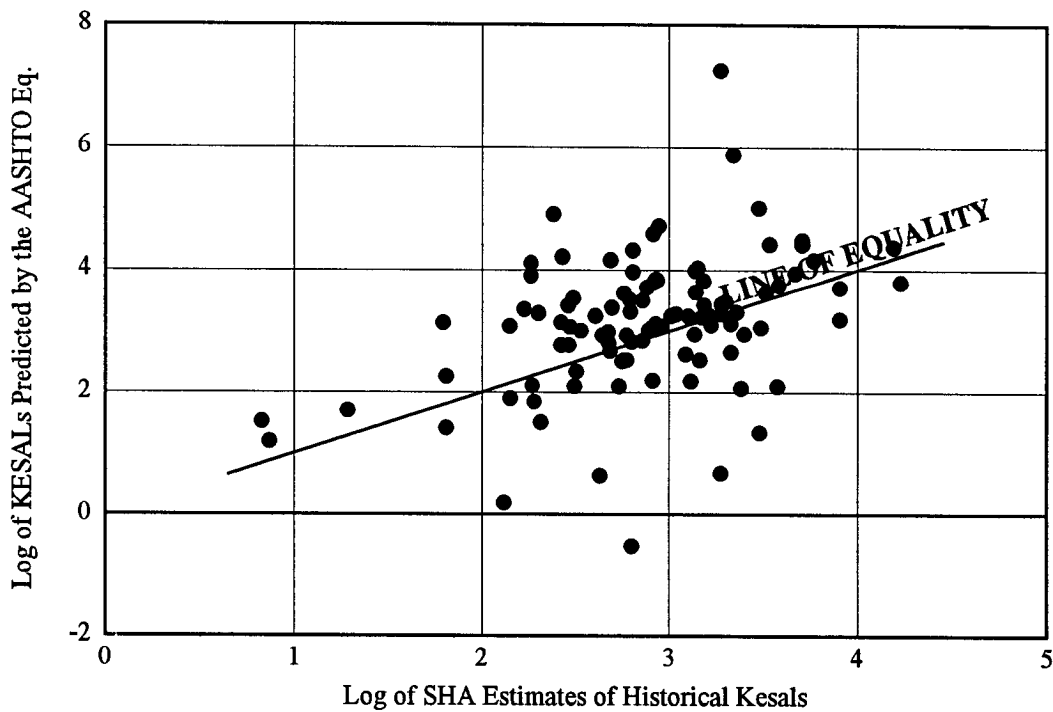


Figure 3. Plot of Predicted Versus Actual KESALs Based on Subgrade Resilient Moduli From Laboratory Testing for 106 Test Sections

$$G_t = \beta(\log W_t - \log \rho) = \log \left(\frac{4.5 - p_t}{4.5 - 1.5} \right) \quad (3)$$

where	G_t	=	the logarithm of the ratio of loss in serviceability at time t to the potential loss taken to a point where serviceability equals 1.5
	β	=	a function of design and load variables that influence the shape of the p-versus-W serviceability curve
	W_t	=	cumulative 18 kip (80kN) ESALs applied at end of time t
	ρ	=	a function of design and load variables that denotes the expected number of axle load applications to a terminal serviceability index
	$\log \rho$	=	$7.35 \log (D+1) - 0.06$
	D	=	slab thickness, in.
	4.5	=	mean initial serviceability value of all sections
	p_t	=	terminal serviceability

In the 1986 and 1993 AASHTO Design Guides, the PCC pavement design model is given as follows:

$$\log W_{18} = Z_R S_o + 7.35 \log (D+1) - 0.06 + \frac{\log \left(\frac{\Delta \text{PSI}}{4.5 - 1.5} \right)}{1 + \frac{1.624 * 10^7}{(D+1)^{8.46}}} + (4.22 - 0.32 p_t) \log \left(\frac{S'_c C_d (D^{0.75} - 1.132)}{215.63 J (D^{0.75} - \frac{18.42}{(E/k)^{0.25}})} \right) \quad (4)$$

where	ΔPSI	=	loss of serviceability ($p_i - p_t$)
	D	=	thickness of PCC pavement, in.
	S'_c	=	modulus of rupture of concrete, psi
	C_d	=	drainage coefficient
	E_c	=	elastic modulus of concrete, psi
	k	=	modulus of subgrade reaction, psi/in.
	J	=	joint load transfer coefficient
	W_{18}	=	cumulative 18 kip (80kN) ESALs at end of time t
	p_i	=	initial serviceability
	p_t	=	terminal serviceability

Five sets of analyses were performed individually for GPS-3, GPS-4, and GPS-5 experiments to examine the ability of the equations to predict the amount of traffic actually sustained by each test section. Initially, analyses were conducted on all available data for each experiment. Then the data sets for each pavement type (JPCP, JRCP, and CRCP) were further separated by four environmental zones. Analyses were then performed for each of the environmental zones for each pavement type.

The predicted KESALs (1000 ESALs) were plotted against the estimated KESALs to display the scatter of the data. The results were also presented in bar graphs to show the ratio of predicted to actual KESALs.

As an example, the plot of predicted versus actual KESALs determined with the original AASHTO model (Equation 3) appears in Figure 4 for JPCP and JRCP. If the predictions were unbiased for all regions, approximately 50% of the points would lie on each side of the line of equality.

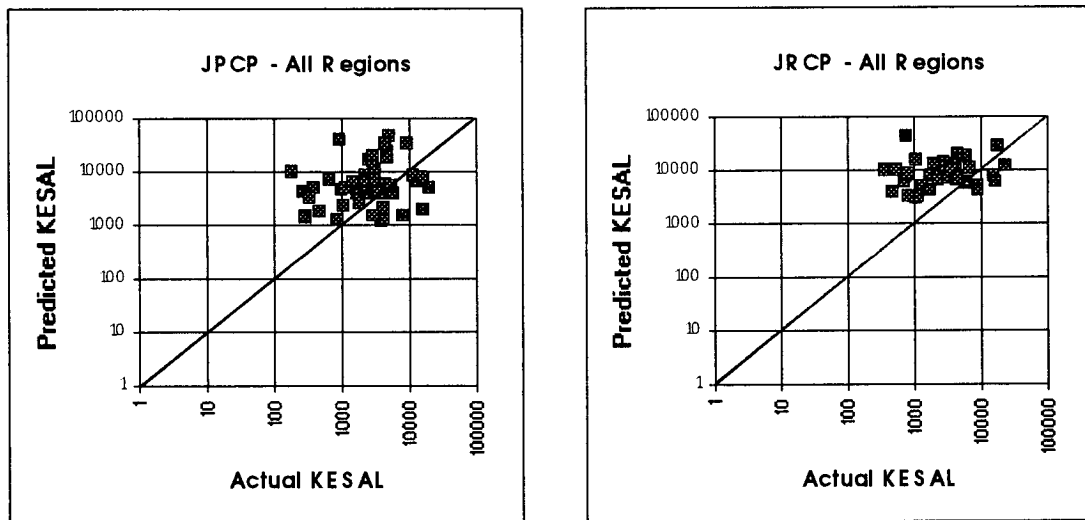


Figure 4. Predicted KESALs Versus Actual KESALs for JPCP and JRCP Determined With the Original AASHTO Prediction Model.

It can be seen that the original AASHTO model overpredicts KESALs for a majority of the test sections (78% of JPCP and 82% of JRCP) and that the overpredictions ranged as high as sixteen times the actual number of KESALs. Similar scatter plots were developed for the separate environmental zones.

The predicted versus actual KESALs plots for JPCP, JRCP, and CRCP determined with the 1993 AASHTO model are shown in Figure 5. The 1993 model predicted much better than the original AASHTO model for these analysis data sets, which suggests that the addition of several design factors considerably improved the performance prediction capability of the model by reducing the bias. However, there is major scatter about the lines of equality, even on these log-log plots. This scatter may be the result of several causes, including

inadequacies in the model, errors in the inputs, and random performance variations (or pure error). Similar plots were prepared and evaluated for JPCP and CRCP pavements.

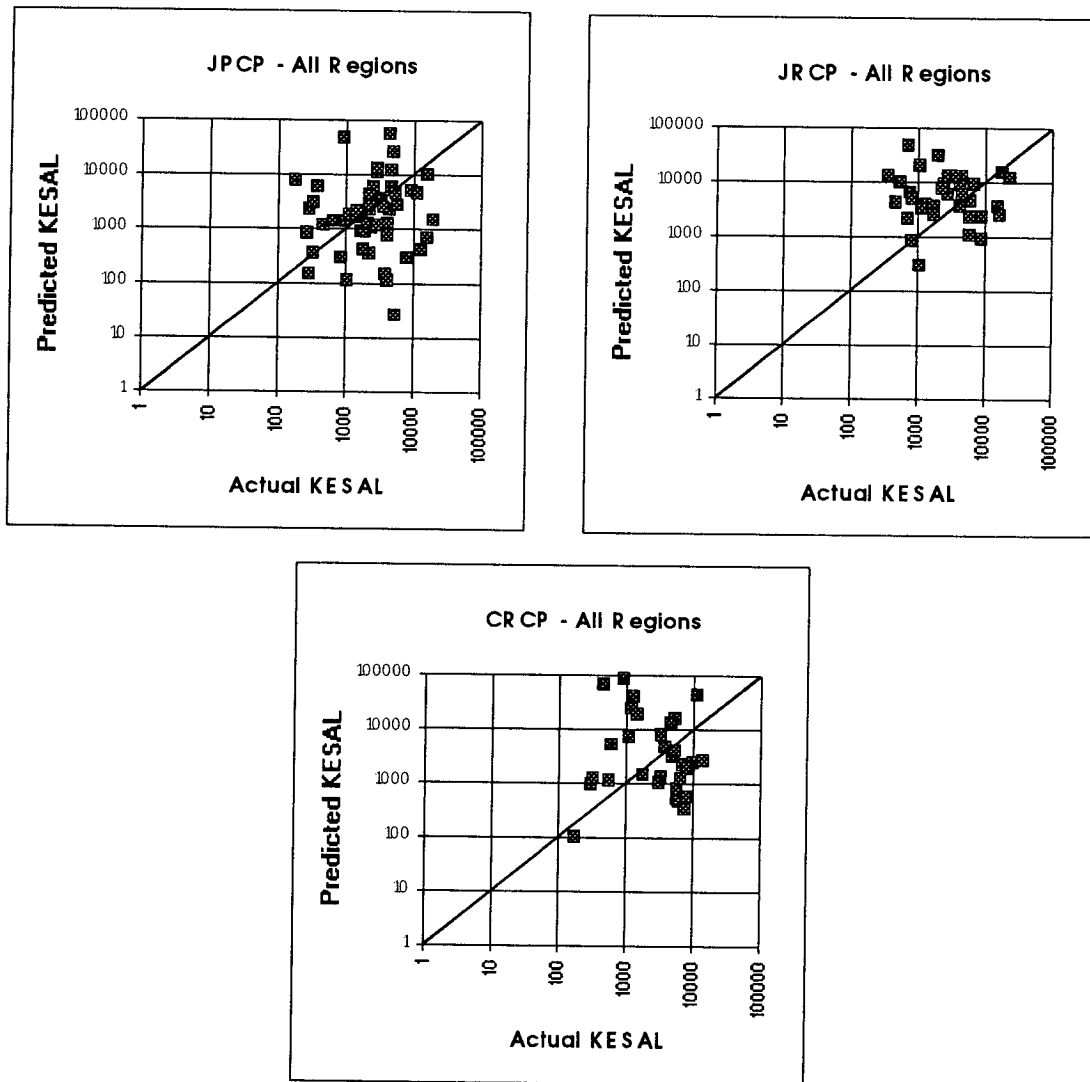


Figure 5. Predicted KESALs vs. Actual KESALs for JPCP, JRCP, and CRCP Determined With the 1993 AASHTO Prediction Model

To analytically determine the ability of the AASHTO concrete pavement design model to predict the actual KESALs observed for the pavement sections, a statistical procedure was followed that determines whether two sample data sets (actual and predicted) are from the same population. The paired-difference method, which uses the student t-distribution, was used to determine if the KESALs as predicted by the AASHTO equation are statistically from the same population as the actual measured KESALs.

Microsoft® EXCEL™ statistical analysis tools were used to compare the observed KESALs to those predicted by the AASHTO equations. The calculated t-statistic (t-calc) is compared to a tabulated t-statistic (t-table) for a specific confidence level. If t-calc is greater than t-table, then the null hypothesis (that they are from the same population) is rejected with a 5% chance of error, since the confidence level selected for this analysis is 95%.

It was observed that t-calc is greater than t-table for one-half the data sets when the original AASHTO model was used, which indicates that the original AASHTO model does not reliably predict the ESALs actually sustained by the pavement sections. However, for the 1993 AASHTO model, the results show that the null hypothesis is not rejected. This finding holds true for all environmental zones. These results show that the improvements to the original AASHTO model were beneficial in increasing the accuracy of the design equation.

Also comparison was made of the actual KESALs to the predicted KESALs at a particular level of design reliability. It was found that the mean $\log W_{50\%}$ prediction is reduced by $Z_R S_o$ (where $Z_R = 1.64$ for 95% reliability, and $S_o = 0.35$). The predicted (at 95% reliability) versus actual KESALs were plotted. Most of the points were below the line of equality, indicating that the consideration of design reliability definitely results in a large proportion of sections (77%) having a conservative design—which is desired. A statistical test was also conducted as before.

The results of these studies were then summarized. The 1986 (or 1993) model appears to provide more or less unbiased predictions in that the plots of predicted to actual KESALs tend to center on the lines of equality. Although the scatter is not very apparent on the log-log plots necessary to include all the points, the actual scatter is major when reviewed arithmetically. Thus, even though collectively the adjustments to the 1993 model seem to have improved prediction capabilities in comparison to the original AASHTO model, the evaluation points to the need for further improvements to increase the precision of the predictions.

Improved Design Equations—Applications and Limitations

It became apparent early in the research that the preponderance of the highway community was not interested in continuing use of the composite index called Present Serviceability Index for design. The preference was for separate design equations for the several significant distress types, so that they could be used both for pavement management and for balanced designs to minimize the distresses individually. This approach was followed in this research.

For any proposed pavement structure, the key distress and roughness indicators are predicted based on the best available LTPP models (from sensitivity analyses described later) over the design traffic and life. The adequacy of the design is judged by the predicted performance in terms of individual distresses, including roughness. Design modifications can be made if any aspect of performance is found to be deficient. This

sequence can then be repeated until an acceptable design is obtained. Examples will be provided.

HMAC Pavements

The distress types considered to be significant were alligator cracking, rutting, transverse (or thermal) cracking, increases in roughness, and loss of surface friction. However, alligator fatigue cracking could not be studied at this early stage because only eighteen pavements displayed medium- or high-severity alligator cracking, and the data collected were not considered adequate for modeling loss of surface friction.

The original intent was to rearrange the models developed for the sensitivity analyses as design equations, but separate consideration of hot mix asphalt concrete (HMAC) and unbound base thicknesses was problematical because the separate effects for some distress types and environmental zones were not additive. That is, increasing the thickness of one layer did not necessarily result in a decreased required thickness for the other. Consequently, it was decided to use structural number, in lieu of HMAC and unbound base thicknesses separately, to develop models that behaved better.

The models were developed again with structural number, but the results discussed above are still reflected in the design models. These models for separate environmental zones had values of adjusted R^2 that varied from 0.69 to 0.88, and they are similar in format to the example in Table 4 (see Sensitivity Analyses and Results).

Figure 6 is an attempted design nomograph to limit roughness in the dry-freeze zone. Two examples are shown on Figure 6 that differ only in the number of ESALs, "N." Both examples limit changes in International Roughness Index (IRI) to 100 in./mi. (159 mm/km), assuming air voids of 5%, AC-10 asphalt, a freeze index of 500, and an average of 70 days each year with temperatures greater than 90°F (32°C). The unexpected result, however, is that the structural number required for 1 million ESALs is 11, while that for 10 million ESALs is 5.1. The immediate response to such a result is that something is wrong with the nomograph or the equation. The nomograph is correct for the equation, so that leaves the equation (with an adjusted R^2 of 0.88) in question. Or could it be that the pavements are trying to communicate something that we do not yet understand?

Because the approach of rearranging the regression equations and establishing limiting levels of distress was not working, it was decided to simply use the equations directly to predict distresses for several trial designs. To explore this approach, a factorial experiment was initiated for HMAC over granular base pavements to study predicted distresses over a range of pavement structures and ESALs (ages for transverse cracking), with material properties fixed at reasonable values and climatic variables set at their regional means. This step required 144 solutions each for predictions of rut depths, changes in IRI, and transverse crack spacing. The results for changes in roughness appear in Table 1. If the goal was to restrict increases in IRI to 100 in./mi. (161 mm/km), it appears that this value would not be experienced until large volumes of ESALs had accumulated, except in the

dry-freeze zone (same zone considered in Figure 6). In this zone, considerable roughness was predicted for pavements with thick base layers before 6 million ESALs had been experienced.

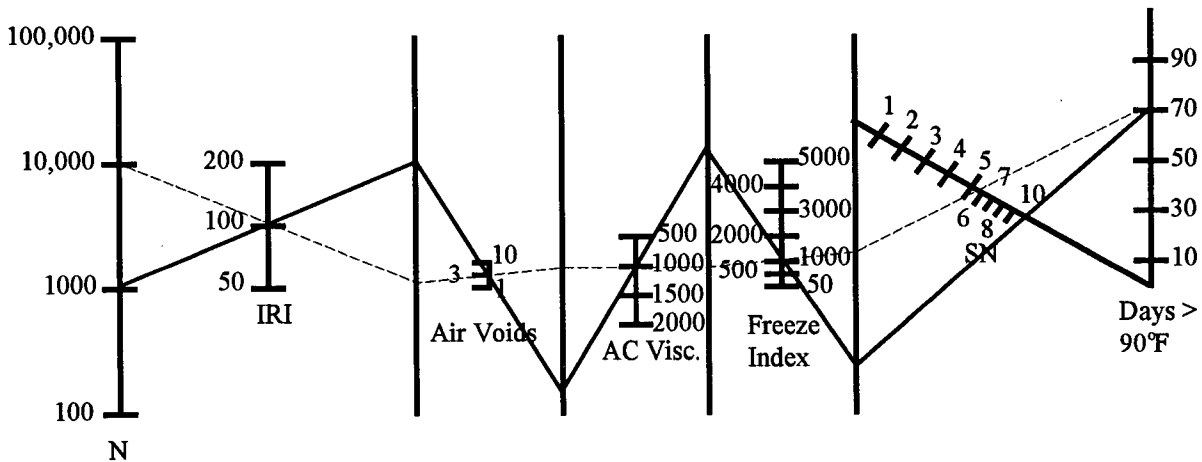


Figure 6. Design Nomograph to Limit Roughness in the Dry-Freeze Zone

The research staff was unable to satisfactorily explain why increasing base thickness in the dry-freeze zone appears to increase potential roughness, which was also strongly indicated by the sensitivity analyses. If it is assumed that the base compaction provided for these pavements was insufficient or later deteriorated because of environmental or other effects, then increasing depths of base could result in more differential rutting and thus roughness. Future studies should be conducted to gain understanding of unexpected results, such as in this example.

While these models may over time prove to be reasonable, they are based for this early analysis on limited time sequence data (generally an initial point and another in 1990 or 1991 for the distresses) and should be used with care and only as design checks in concert with other design procedures. While a good distribution of pavement ages undoubtedly help in explaining "curvature" in the relationships, which will be enhanced by future time sequence data, the research staff does not wish to promote these models for design use at this time.

The results for rut depth and transverse crack spacing from the factorial experiment discussed above appear in *Evaluation of the AASHTO Design Equations and Recommended Results* (SHRP-P-394), along with more discussion.

Table 1. Predicted Change in Roughness in In./Mi. Based on Regional Predictive Equations, Ranges of Layer Thicknesses and ESALs, With Climatic Data at Their Regional Means, HMAC Over Granular Base (Also Predictive Equation Statistics)

HMAC Thickness, In.	Base Thickness, In.	ESALs in Millions and Environmental Zones																			
		Wet-No Freeze					Dry-No Freeze					Wet-Freeze					Dry-Freeze				
		1	6	12	25		1	6	12	25		1	6	12	25		1	6	12	25	
2	8	55	80	92	107	26	53	71	95	28	43	52	62	31	50	60	73				
	16	28	40	46	54	14	29	39	52	27	42	50	60	48	77	93	114				
	24	14	20	23	27	8	16	21	28	26	41	49	58	74	120	145	177				
6	8	28	25	47	55	12	25	33	44	39	61	73	87	30	49	59	72				
	16	14	21	24	29	7	14	18	24	38	59	71	85	47	76	92	112				
	24	7	10	12	14	4	7	10	13	37	58	69	82	73	119	143	175				
10	8	14	21	24	28	6	12	15	21	46	72	85	103	30	49	58	71				
	16	7	11	12	14	3	6	8	11	45	70	83	100	46	75	91	111				
	24	4	5	6	7	2	3	5	6	43	68	80	97	72	117	141	173				
	R ²	0.85					0.95					0.87					0.94				
	Adj. R ²	0.81					0.93					0.84					0.92				
	RMSE in Log Δ IRI2	0.31					0.18					0.27					0.21				

Note: Fixed values of variables: HMAC air voids = 5%
 HMAC Aggregate < #4 sieve = 55%
 AC viscosity = 1000 poise
 Base compaction = 95% modified AASHTO
 Asphalt content = 5%
 Subgrade soil < #200 sieve = 20%

1 in. = 25.4 mm

PCC Pavements

The same approach described above for HMAC pavements was used for portland cement concrete (PCC) pavements, and the same limitations on the quality of models apply. The distress models described previously for the sensitivity analyses may be used as design checks for PCC pavements.

The following presentation illustrates the potential use of distress models for evaluating or developing pavement designs. Future versions of these models should be greatly improved and should be adequate for use in design. A JRCP design has been proposed, based on an agency's standard design procedures and design standards. The values selected for the required design inputs for the LTPP models are summarized below:

Design life:	30 years
Traffic:	30 million ESALs in design lane
Climate:	PRECIP = 30 in. (762 mm)
	TRANGE = 60°F (33.3°C)
Subgrade:	KSTATIC = 300 psi/in. (82.7 Kpa/mm)
Base:	treated granular material (asphalt or cement)
Slab:	THICK = 9 in. (229 mm)
	PSTEEL = 0.12% area
Joints:	JTSPACE = 40 ft (12 m)
	DOWDIA = 1.25 in. (32 mm)
Shoulders:	AC EDGESUP = 0

These pavement design inputs and characteristics were utilized with all of the JRCP predictive models to estimate performance over the 30-year design life and beyond. (Note that prediction beyond about 20 years exceeds the inference space for the current LTPP models.) Joint faulting, joint spalling, transverse crack deterioration, and IRI were predicted. Since some readers may not be familiar with the values of the IRI, the corresponding Present Serviceability Rating (PSR) has been estimated based on a recently developed model from user panel data. The results are shown in Table 2. Some interesting results are summarized:

- Faulting of only 0.10 inch (2.5 mm) was predicted at 30 years. A level of approximately 0.25 inch (6.4 mm) is critical from a roughness standpoint for a JRCP with long joint spacing. Thus, joint load transfer is adequate over the 30-year period.
- Joint spalling (converted from percentage of joints deteriorated to number of joints per mile) is predicted to increase rapidly after 15 years until at 30 years about 106 joints per mile (67 joints/km) have deteriorated. Joint repair will be required after about 15 to 20 years to keep the pavement in service unless some improvement in joint design is made.

Table 2. Use of LTPP Predictive Models for Evaluating a JRCP Design Example.

Age	CESAL	JT Space	K Static	Edge SPRT	Dowel DIA	% Steel	Temp	Rain	THCK	FLT	Spall	CRCK	IRI	PSR
Yrs	10 ⁶	ft	psi/in.	*	in.	%	°F	in.	in.	in.	joints/mi	crck/mi	in./mi	**
5	5	40.0	300	0	1.25	0.12	60	30	9	0.01	0***	0***	69	3.8
6	6	40.0	300	0	1.25	0.12	60	30	9	0.01	0	0	70	3.8
7	7	40.0	300	0	1.25	0.12	60	30	9	0.01	0	0	71	3.7
8	8	40.0	300	0	1.25	0.12	60	30	9	0.02	0	0	72	3.7
9	9	40.0	300	0	1.25	0.12	60	30	9	0.02	0	0	72	3.7
10	10	40.0	300	0	1.25	0.12	60	30	9	0.02	0	0	73	3.7
15	15	40.0	300	0	1.25	0.12	60	30	9	0.03	21	0	78	3.6
20	20	40.0	300	0	1.25	0.12	60	30	9	0.05	46	7	82	3.6
25	25	40.0	300	0	1.25	0.12	60	30	9	0.07	74	17	86	3.5
30	30	40.0	300	0	1.25	0.12	60	30	9	0.10	106	26	90	3.5
40	40	40.0	300	0	1.25	0.12	60	30	9	0.17	176	45	99	3.3
50	50	40.0	300	0	1.25	0.12	60	30	9	0.28	256	64	107	3.2

*EDGESUP = 1 for tied PCC shoulder, = 0 for any other shoulder type.

$$**PSR = 5 * e^{(-0.0041*IRI)} \quad (1).$$

***Negative values were set at zero.

Note: 1 in. = 25.4 mm; 1 ft = 0.3 m; 1 psi/in. = 275.6 Pa/mm

- Transverse crack deterioration is relatively low over most of the 30-year design period. However, crack deterioration increases greatly at about 30 years, requiring considerable repair. An increased amount of reinforcement would reduce the amount of crack deterioration as subsequently shown.
- The IRI remains within an acceptable range over the 30-year design period as indicated by the PSR values.

Evaluation of the 1993 AASHTO Overlay Design Equations

The 1993 revisions to the AASHTO overlay design procedure were intended to provide overlay thicknesses that address a pavement with a structural deficiency. A structural deficiency arises from any condition that adversely affects the load-carrying capability of the pavement structure. Such conditions include inadequate thickness, as well as cracking, distortion, and disintegration.

The AASHTO pavement overlay design procedures are based on the concept that time and traffic loading reduce a pavement's ability to carry loads. An overlay is designed to increase a pavement's ability to carry loads over a future design period. The required structural capacity for a PCC or HMAC pavement to successfully carry future traffic is calculated, with the appropriate AASHTO 1993 new pavement design equation. The effective structural capacity of the existing pavement is evaluated with procedures for overlay design presented in the Guide. These procedures can be based on a visual survey and material testing results, or on results of nondestructive testing (NDT) of the existing pavement. An overlay is then designed based on the structural deficiency represented by the difference between the structural capacity required for future traffic and the structural capacity of the existing pavement.

LTPP data from GPS-6A, GPS 6-B, GPS-7A, GPS-7B, and GPS-9 experiments were used to evaluate the 1993 version of the AASHTO overlay design equations. While data on design life and levels of reliability sought were not available, a limited set of test sections were identified that had sufficient data to support limited evaluations. These sections included nine with HMAC overlays of HMAC, five with HMAC overlays of PCC, and six with unbonded PCC overlays of PCC. Even for these test sections, it was necessary to use existing data to estimate values for some of the inputs to the design equations. Procedures used for estimating specific input values are described in *Evaluation of the AASHTO Design Equations and Recommended Improvements* (SHRP-P-394).

The design equations were then used to predict the overlay thicknesses required, and these thicknesses were compared to the thicknesses of the overlays actually constructed. The results from recent profile measurements and distress surveys were also used to evaluate the adequacy of the AASHTO design equation to establish an appropriate design overlay thickness. A summary of the results from these comparative evaluations appears in Table 3.

Although these evaluations were seriously constrained by data limitations, the equation appears to work quite well for this small data set of five test sections of HMAC overlays of PCC. The evaluations were generally inconclusive for HMAC overlays of HMAC and unbonded PCC overlays of PCC.

Additional data will be available in the future for comparative evaluations regarding the design periods and levels of reliability used for design of overlays. Conclusive evaluations are probably not possible without this information if comparisons are to be made on the same design basis.

Table 3. Results From Comparative Evaluation of 1993 AASHTO Overlay Equations

Test Section Number	Type of Pavement	Results From Comparisons			
		Conservative	Adequate	Inadequate	Inconclusive
016012	AC/AC		X		
016109	"				X
351002	"				X
356033	"				X
356401	"		X		
486079	"		@95% Reliability		
486086	"				X
486160	"	X			
486179	"				X
Subtotals for AC/AC		1	3	0	5
087035	AC/PCC		X		
175453	"		X		
283097	"		X		
287012	"		X		
467049	"			X	
Subtotals for AC/PCC		0	4	1	0
69049	PCC/PCC			X	
89019	"				X
89020	"				X
269029	"				X
269030	"				X
489167	"				X
Subtotals for PCC/PCC		0	0	1	5
Totals		1	7	2	10

Sensitivity Analyses and Results

"Sensitivity analysis" does not have an established meaning for either research engineers or statisticians, but it has come to have a specific meaning to some individuals from both disciplines. The definition as applied to this research follows:

Sensitivity analyses are statistical studies to determine the sensitivity of a dependent variable to variations in independent variables (sometimes called explanatory variables) over reasonable ranges.

There is no single method of conducting sensitivity analyses, but they all require a reasonably accurate equation (or model) for predicting distress. The procedures used for the studies reported involved setting all explanatory variables in a predictive equation at their means and then varying each one independently from one standard deviation above the mean to one standard deviation below the mean. The relative sensitivity of the distress prediction for that variable is the change in the predicted distress across the range of two standard deviations. This range is compared to the changes that occur when other explanatory variables were varied in the same manner.

Sensitivity Analyses for HMAC Pavements

It became apparent early that predictive models developed from the entire database, whose inference space included all of the United States and parts of Canada, would not generally result in satisfactory models for conducting the sensitivity analyses. Consequently, where sufficient test sections displaying the distress of interest were available, databases were formed for each of the four environmental zones and separate predictive models developed. Regional models were not possible for PCC pavements because the resulting databases were too small.

The regional models for HMAC pavements have values of the adjusted coefficient of determination R^2 ranging from 0.65 to 0.93. As an example, the model developed for prediction of rutting in the wet-freeze environmental zone appears as Table 4. The form of the equation appears at the top of the table. The explanatory variables or interactions appear in the table, along with the coefficients that provide the details of the equation. As can be seen, the exponents B and C are calculated by multiplying the explanatory variables or interactions in the left column by the regression coefficients b_i and c_i and adding the results. For example, the constant b_1 for this model is 0.183, and is equal to B because all the other values of b_i are 0. To calculate C, the constant term is 0.0289, the log of air voids in HMAC is multiplied by -0.189, etc. The results of the sensitivity analyses conducted with this predictive equation appear in Figure 7a. From Figure 7a it can be seen that the strongest impact on the occurrence of rutting in the wet-freeze zone may be expected to be the number of KESALs (1000 equivalent single axle loads). The dashed lines and arrow to the left indicate that reductions in KESALs decrease rutting, but the standard deviation for KESALs is greater than the mean and negative KESALs are not possible. Freeze index is the next most important, followed by the percentage of the

HMAC aggregate passing a #4 sieve, air voids, and so on. It can also be seen from the directions of the arrows that increasing KESALs and freeze index may be expected to increase rut depths, while increasing amounts of aggregate passing the #4 sieve, air voids, and asphalt thickness may be expected to decrease rutting.

Table 4. Coefficients for Regression Equations Developed to Predict Rutting in HMAC on Granular Base for the Wet-Freeze Data Set

Rut depth = $N^B 10^C$
(In.)

Where:

N = Number of Cumulative KESALs

B = $b_1 + b_2 x_1 + b_3 x_2 + \dots + b_n x_{n-1}$

C = $c_1 + c_2 x_1 + c_3 x_2 + \dots + c_n x_{n-1}$

Explanatory Variable or Interaction (x_i)	Units	Coefficients for Terms In	
		b_i	c_i
Constant Term	--	0.183	0.0289
Log (Air Voids in HMAC)	% by Volume	0	-0.189
Log (HMAC Thickness)	Inches	0	-0.181
Log (HMAC Aggregate #4 Sieve)	% by Weight	0	-0.592
Asphalt Viscosity at 140°F (60°C)	Poise	0	1.80×10^{-5}
Log (Base Thickness)	Inches	0	-0.0436
(Annual Precipitation * Freeze Index)	Inches Degree-Days	0 0	3.23×10^{-6}

n = 41 $R^2 = 0.73$ Adjusted $R^2 = 0.68$ RMSE in \log_{10} Rut Depth = 0.19

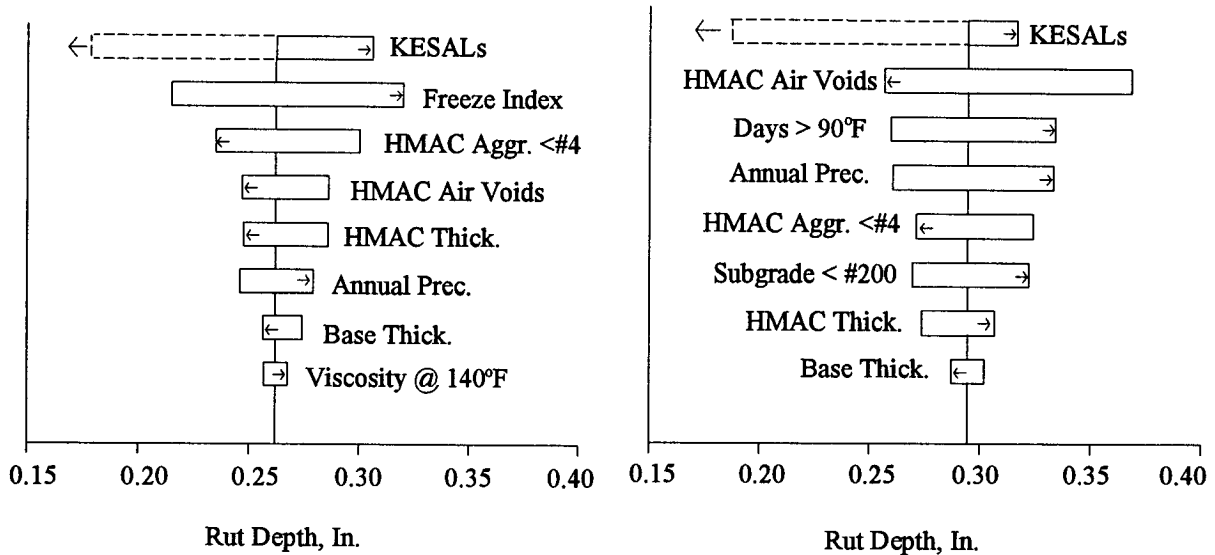


Figure 7. Results From Sensitivity Analyses for Rutting in HMAC on Granular Base

In order to illustrate how different the sensitivities may be from one environmental zone to another, the sensitivity analysis results for the dry-no freeze zone are included as Figure 7b. As can be seen, the majority of the variables are the same as for the wet-freeze zone, but there are some differences and the relative levels of sensitivities vary between environmental zones. Similar studies were conducted for rutting in other environmental zones and for increase in roughness and transverse crack spacing in all four environmental zones.

Summary of Sensitivity Analysis Results for HMAC Pavements

The twelve most significant variables from the sensitivity analyses for HMAC pavements are listed below by distress type, in order of relative ranking with the most significant variable at the top and the least at the bottom.

<u>Rutting</u>	<u>Change in Roughness</u>	<u>Transverse Cracking</u>
KESALs	KESALs	Age
Air Voids in HMAC	Asphalt Viscosity	Annual Precipitation
HMAC Thickness	Days With Temp. > 90°F	HMAC Thickness
Base Thickness	(32°C)	Base Thickness
Subgrade < #200 Sieve	HMAC Thickness	Asphalt Viscosity
Days With Temp. > 90°F	Base Thickness	Base Compaction
(32°C)	Freeze Index	Freeze Index
HMAC Aggregate	Subgrade < #200 Sieve	Days With Temp. >
< #4 Sieve	Air Voids in HMAC	90°F (32°C)
Asphalt Viscosity	Base Compaction	Subgrade < #200 Sieve
Annual Precipitation	Annual Precipitation	KESALs
Freeze Index	Daily Temp. Range	Annual Freeze-Thaw
Base Compaction	Annual Freeze-Thaw Cycles	Cycles
Average Annual Min.		HMAC Aggregate < #4
Temp.		Sieve

It can be seen that nine of these variables are significant for all three distress types. The exceptions are as follows:

- Air voids in HMAC were not significant for transverse cracking.
- HMAC aggregate passing a #4 sieve was not significant for change in roughness.
- The annual number of freeze-thaw cycles was not significant for rutting.
- Average annual minimum temperature and daily temperature range were significant only for rutting and change in roughness, respectively.

It can also be seen that four environmental variables were found to be significant for rutting, five for change in roughness, and four for transverse cracking.

Some tentative comments that result from the sensitivity analyses follow:

- Most of the rutting appears to have occurred in these pavements soon after they were opened to traffic.
- The HMAC aggregate passing the #4 sieve was selected to represent the effects of gradation. Within its inference spaces in the separate data sets, increasing amounts of aggregate passing the #4 sieve appeared beneficial in reducing rutting.
- As expected, traffic loading is the strongest contributor to the occurrence of rutting and roughness, and pavement age had the strongest effect on transverse cracking. (It should be remembered that pavements were generally designed and constructed to limit the occurrence of rutting and roughness, so the relative significances for the variables may apply only to such pavements.)
- Thicker HMAC surfaces and granular base layers may be expected to generally decrease all three types of distress (again expected).

Some results are difficult to explain. For example, the studies indicate that increasing base compaction, annual precipitation, asphalt viscosity, or annual freeze-thaw cycles (or freeze index) tends to increase transverse crack spacing (reduce cracking).

In summary, most results from the sensitivity analyses for HMAC pavements appear reasonable; however, others are surprises that (1) may have resulted from the specific characteristics of the data sets on which they are based, (2) represent mechanisms we do not yet understand, (3) result from interactions not explained by the equation forms, or (4) derive from other causes.

Sensitivity Analyses for PCC Pavements

For PCC pavements, equations to predict the occurrence of distresses were developed using entire LTPP databases and sensitivity analyses carried out in the same manner. Because it was not possible to develop regional models, the value of R^2 varied from 0.34 to 0.78. The sensitivity analysis for PCC pavements is illustrated below for joint faulting.

The final model for doweled transverse joint faulting is as follows:

$$\begin{aligned}
\text{FAULTD} = \text{CESAL}^{0.25} * & \left[0.0238 + 0.0006 * \left(\frac{\text{JTSPACE}}{10} \right)^2 \right. \\
& + 0.0037 * \left(\frac{100}{\text{KSTATIC}} \right)^2 + 0.0039 * \\
& \left. \left(\frac{\text{AGE}}{10} \right)^2 - 0.0037 * \text{EDGESUP} - 0.0218 * \text{DOWDIA} \right] \quad (5)
\end{aligned}$$

where

FAULTD	=	mean transverse doweled joint faulting, in.
CESAL	=	cumulative 18,000-pound (80 kN) ESALs in traffic lane, millions
JTSPACE	=	mean transverse joint spacing, ft
KSTATIC	=	mean backcalculated static k-value, psi/in.
AGE	=	age since construction, years
EDGESUP	=	edge support, 1 if tied concrete shoulder, 0 any other shoulder type
DOWDIA	=	diameter of dowels in transverse joints, in.

Statistics	N	=	59 sections
	R ²	=	0.534
	RMSE	=	0.028 in. (0.7 mm)

The results of the sensitivity analysis shown in Figure 8 show that CESALs, joint spacing, age, and the static k-value have the greatest effects on doweled joint faulting, and increases in the significant variables appear to result in logical increases or decreases in the dependent variable.

Predicted faulting increases with increasing CESALs, joint spacing, and age. An increase in static k-value, which shows the effect of subgrade stiffness on the development of faulting, results in a decrease in faulting. Edge support provided by a tied concrete shoulder also causes a slight reduction in faulting. In addition, faulting decreases as dowel diameter increases, which reflects the reduction in dowel/concrete bearing stress brought about by the use of larger dowel bars.

Three-dimensional plots of the response surface of this model generated to show the predicted relationship between faulting and CESALs and age and joint spacing are shown in Figures 9 and 10. As CESALs increase, faulting increases rapidly at first and then the rate of increase decreases. Faulting also increases with age and as joint spacing increases.

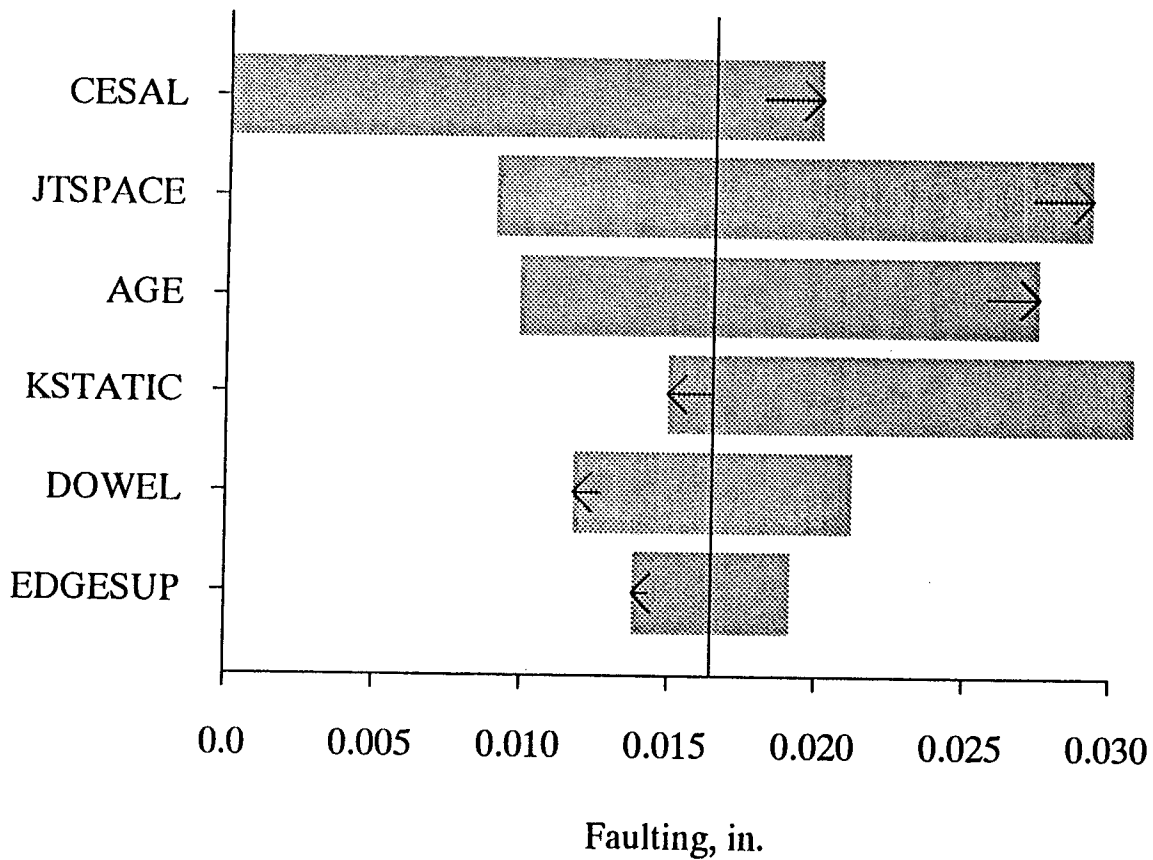


Figure 8. Sensitivity Analysis for Doweled Joint Faulting Model

Summary of Sensitivity Analysis Results for PCC Pavements

Table 5 lists the rankings for individual explanatory (independent) variables, in terms of relative sensitivities, for each of the ten separate models and sensitivity analyses. One column indicates the number of models for which a specific explanatory variable was significant. The last column to the right gives average rankings; a rank of 8 was arbitrarily assigned when the variable was not significant. The number of explanatory variables ranged from 2 to 6 per model, with a mean of 4.1, so the assigned priority had to be greater than 6. Because there could be other relatively nonsignificant variables that have stronger impacts on the occurrence of distress, a value of 8 appeared logical.

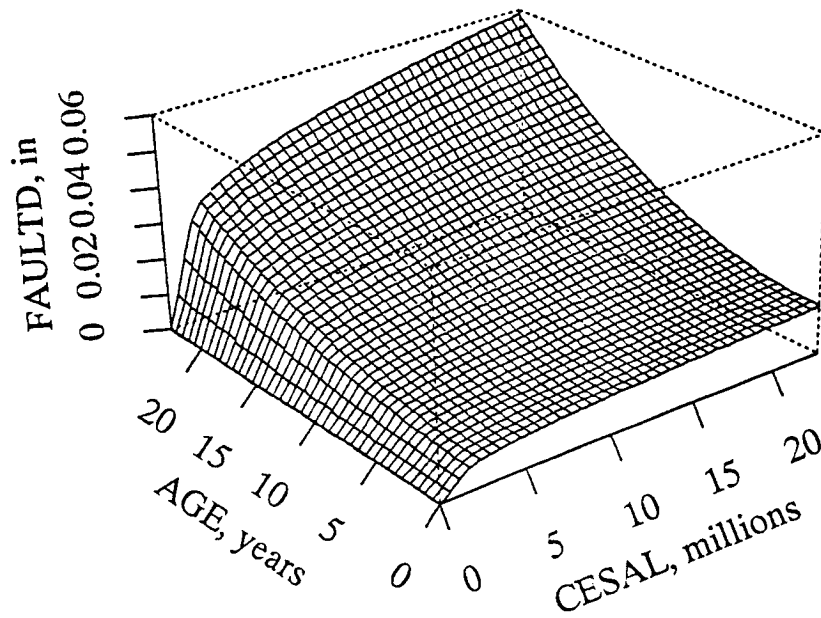


Figure 9. Three-Dimensional Plot (FAULTD, AGE, CESAL) of Doweled Joint Faulting Model

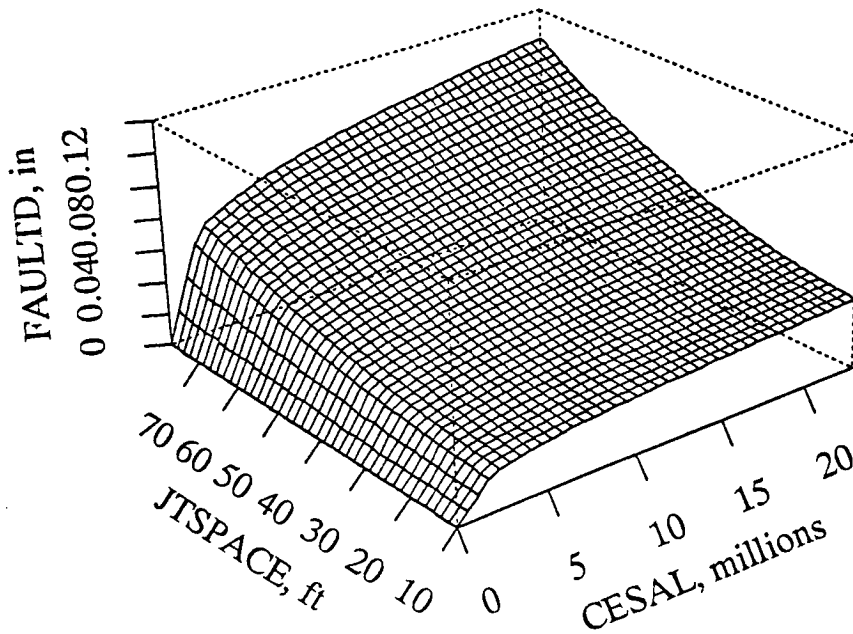


Figure 10. Three-Dimensional Plot (FAULTD, JTSPACE, CESAL) of Doweled Joint Faulting Model

Table 5. Significance Rankings for Explanatory Variables, by Distress Type and Pavement Type, for PCC Pavements

Explanatory Variables	Joint Faulting JCP w/ Dowels	Joint Faulting JCP w/o Dowels	Transverse Crack Deterioration, JPCP	Transverse Crack Deterioration, JRCP	Joint Spalling, JPCP	Joint Spalling, JRCP	IRI, JPCP w/ Dowels	IRI, JPCP w/o Dowels	IRI, JRCP w/o Dowels	IRI, CRCP	No. Models Significant	Average Ranking
CESALS	1	1		3				1		4	5	5.0
Joint Spacing	2						1				2	6.7
Age	3	2			2	1	4		4		6	4.8
Static k-Value	4			1			5		2		4	5.9
Dowel Diameter	5										1	7.7
Edge Support	6						3		3		3	6.8
Precipitation		3		4				2	5		4	6.2
Freeze Index		4									1	7.6
Longitudinal Subdrainage		5									1	7.7
Slab Thickness			1				2		1	5	4	5.7
PCC Flexural Strength			2								1	7.4
Percent Steel				2						1	2	6.7
Annual Freeze-Thaw Cycles					1			3			2	6.8
Monthly Temperature Range						2					1	7.4
Type of Subgrade (Granular or Clay)								4		2	2	7.0
Type of Base (Treated or Untreated)								5			1	7.7
Traffic Lane (Widened or Not)										3	1	7.5

Note: Empty Cells are considered as 8 for averaging.

The most significant independent variables are listed below in order of combined rankings. One list is based on average rankings, and one is based on the number of models in which the variable was included (the latter ranking method was used to order the two in case of a "tie"):

<u>Ranking by Average</u>	<u>Ranking by Number of Models Found Significant</u>
Age	Age
CESALs	CESALs
Slab Thickness	Slab Thickness
Static k-Value	Static k-Value
Precipitation	Precipitation
Joint Spacing	Edge Support (Tied Shoulders)
Percentage of Steel	Joint Spacing
Edge Support (Tied Shoulders)	Percentage of Steel
Annual Freeze-Thaw Cycles	Annual Freeze-Thaw Cycles
Type of Subgrade	Type of Subgrade
PCC Flexural Strength	PCC Flexural Strength
Monthly Temperature Range	Monthly Temperature Range
Widened Traffic Lane	Widened Traffic Lane
Freeze Index	Freeze Index
Dowel Diameter	Dowel Diameter
Subdrainage	Subdrainage
Type of Base	Type of Base

The rankings are almost identical for both methods. However, this set of rankings does not tell the whole story; the rankings depend on the type of pavement and the type of distress. Tentative conclusions drawn from the sensitivity analyses (and partially from past experience) are given below.

Tentative Conclusions for JPCP

1. The use of sufficiently sized dowels for the traffic loadings (the larger the dowel diameter the less faulting) will ensure that faulting will not become significant and cause severe roughness in JPCP. Dowel use is particularly important for heavy traffic in cold and wet climates. Thicker slabs by themselves do not reduce faulting significantly. Longitudinal subdrainage will help reduce faulting in non-doweled joints. The use of a tied concrete shoulder will reduce doweled joint faulting.
2. Increased slab thickness has a strong effect on reducing transverse slab cracking and providing a smoother JPCP (lower International Roughness Index [IRI]) over time.

3. The provision of increased subgrade support, as indicated by the backcalculated k-value will result in a lower IRI and a smoother pavement over time and traffic. Increased support over an existing soft subgrade would likely require either deep treatment of the soil or a thick granular layer over the subgrade (not just a treated base layer).
4. The use of shorter slabs for JPCP will reduce the amount of joint faulting and transverse cracking and will result in a smoother pavement (lower IRI) over time.
5. The specification of highly durable concrete in freeze climates is desirable, so that freezing and thawing and other climatic factors do not result in significant joint spalling.

Tentative Conclusions for JRCP

1. The conclusions in Items 1 and 3 for JPCP also hold for jointed reinforced concrete pavement (JRCP).
2. An increased percentage of longitudinal reinforcement will help control the deterioration of transverse cracks.
3. Shorter JRCP slabs will reduce the amount of joint faulting.

Tentative Conclusions for CRCP

1. An increase in the percentage of longitudinal reinforcement will provide a smoother continuously reinforced concrete pavement (lower IRI) over time. An increased percentage of steel will reduce the amount of punchouts and the deterioration of transverse cracks.
2. An increased subgrade support will result in fewer deteriorated transverse cracks and a lower IRI (smoother pavement). Increased support over an existing soft subgrade would likely require either treatment of the soil or a thick granular layer over the subgrade (not just a treated base layer).
3. A widened traffic lane will provide a smoother CRCP (lower IRI) over time.
4. Increased slab thickness will result in a somewhat smoother CRCP (lower IRI) over time, which is probably due to fewer punchouts as a result of the thicker slab.

Recommendations for Future Analyses

One primary objective of this research was to prepare for future analyses when data from many more sections and more time series data would be available. Some of the many products achieved were

- usable databases for combinations of pavement and distress types,
- statistical characterizations of the data,
- identification of biases in the data,
- distress models,
- valuable insight into the need for regional models,
- procedures for developing models from Long-Term Pavement Performance (LTPP) data,
- identification of variables that have significant impact on specific distresses,
- procedures for conducting sensitivity analyses on LTPP data,
- identification of procedures that do not work,
- identification of mechanistic variables and "clusters" for future modeling,
- identification of the shortcomings of the American Association of State Highway and Transportation Officials (AASHTO) design equations,
- identification of potential improvements to the AASHTO design equations, and
- recommendations to follow in future analyses.

Some additional studies not required by the contract, but that the research staff hoped to achieve, were (1) development of mechanistic-empirical models, using mechanistic responses (stresses and strains) from the data analyses conducted by Michigan State University (Contract P-20b), as independent variables in nonlinear regression models and (2) development of separate load equivalence factors for the specific distresses modeled. These studies can be undertaken as more time sequence data becomes available.

Future analytical objectives should include (1) development of distress models for use in design procedures, pavement management, and sensitivity analyses; (2) use of time sequence data to improve the functional forms for new predictive equations; (3) calibration of existing mechanistic-empirical models with LTPP data; (4) combining knowledge from Strategic Highway Research Program (SHRP) studies of asphalt, concrete, and long-term performance to improve performance models and gain additional insight into the effects of independent variables on performance; (5) development of models for layer stiffnesses in terms of component characteristics; (6) followup on unexpected phenomena resulting from analyses; and (7) evaluation of seasonal changes in layer stiffnesses and surface profiles.

A number of different modeling techniques, each with its own set of strengths and weaknesses, were suggested by various experts for future analyses. Techniques that should be considered during future analyses should include (1) those developed for these early analyses, (2) discriminate analysis, (3) methods that use "censored data" (World Bank procedures used in the Brazil Study and others), (4) survival analysis, (5) neural network approaches (relatively new applications to engineering systems), (6) Bayesian analysis, (7) nonlinear regression analysis, (8) advanced modern regression techniques, and (9) mechanistic-based models. Each of these techniques is discussed briefly in *Lessons Learned and Recommendations for Future Analyses* (SHRP-P-680).

As a final comment on future analyses of LTPP data, the processing of data into databases and the analyses for a spectrum of pavement type/distress type combinations and analytical objectives are both time-consuming and expensive. Future analyses should be sufficiently funded to fully harvest the results from the hundred million dollar plus effort undertaken by SHRP, Federal Highway Administration, and the State Highway Agencies.

Overall, these limited early results clearly demonstrate the potential power and usefulness of the LTPP data base. This study is only a small beginning to the enormous possibilities available to improve our design and rehabilitation capabilities.